6-1-2005

Positive spin polarization in $Co/AlO_3/Co$ tunnel junctions driven by oxygen adsorption

Kirill D. Belashchenko
University of Nebraska-Lincoln, belashchenko@unl.edu

Evgeny Y. Tsymbal
University of Nebraska-Lincoln, tsymbal@unl.edu

Ivan I. Oleynik
University of South Florida, oleynik@cas.usf.edu

Mark van Schilfgaarde
Arizona State University, mark.van_schilfgaarde@kcl.ac.uk

Positive spin polarization in $Co/Al_2O_3/Co$ tunnel junctions driven by oxygen adsorption

K. D. Belashchenko and E. Y. Tsymbal
Department of Physics and Astronomy and Center for Materials Research and Analysis, University of Nebraska, Lincoln, Nebraska 68588, USA

I. I. Oleynik
Department of Physics, University of South Florida, Tampa, Florida 33620, USA

M. van Schilfgaarde
Department of Chemical and Materials Engineering, Arizona State University, Tempe, Arizona 85287, USA
(Received 18 January 2005; published 27 June 2005)

Using a first-principles Green's function technique, we study spin-dependent tunneling in two model realizations of (111) fcc $Co/Al_2O_3/Co$ tunnel junctions assuming O-terminated crystalline epitaxy in the corundum structure. For the first model, which includes 3 O atoms at the interface, the tunneling current is polarized negatively, just as for the clean Co surface. The second model contains additional oxygen atoms inside large pores at each interface. Located at the three-fold hollow adsorption sites, these O atoms bind very strongly to Co. This bonding creates an interface band in the majority-spin channel which strongly enhances the tunneling current in this channel. As a result, the spin polarization changes sign and becomes positive, similar to that for the oxidized Co surface studied previously. These results show that the common argument of "mostly *s*-electron tunneling," which is often used to explain the positive spin polarization in $Co/Al_2O_3/Co$ junctions is quantitatively incorrect. In reality, the spin polarization in these junctions is controlled by the interfacial structure and bonding. Moreover, interfacial adsorption of oxygen may be a prerequisite for achieving the positive spin polarization.

DOI: 10.1103/PhysRevB.71.224422 PACS number(s): 72.25.Mk, 73.40.Gk, 73.40.Rw, 73.23.−b

I. INTRODUCTION

Magnetic tunnel junctions (MTJ) have attracted much attention owing to their potential application in magnetic random-access memories and magnetic field sensors (for a recent review of TMR see Ref. 1). The main property of a MTJ is the tunneling magnetoresistance (TMR), which is defined as $R=(G_P-G_{AP})/G_{AP}$ where G_P, G_{AP} are the conductances observed when the ferromagnetic electrodes are magnetized parallel or antiparallel to each other. High values of TMR are beneficial for applications.

If the two electrodes are made of the same material, the TMR is usually positive, because "easy" tunneling channels at each surface match better in the parallel configuration. However, the TMR measurement does not tell anything about the relative contributions of the two spin channels. This information can be obtained in related Meservey-Tedrow experiments where the second electrode is replaced by a superconductor with an induced Zeeman splitting of the bands.[2] In this experiment the *spin polarization* $P=(G_\uparrow-G_\downarrow)/(G_\uparrow+G_\downarrow)$ of the tunneling current is measured directly, where $G_\uparrow$ and $G_\downarrow$ are the conductances associated with majority spin and minority-spin electrons, respectively.

The majority of experiments on spin-polarized tunneling are performed using amorphous Al_2O_3 as the barrier material. The electrodes are fabricated from various ferromagnetic materials including elemental 3-*d* transition metals Fe, Co, and Ni. The spin polarization has been found to be positive for all three ferromagnets. If we assume that the spin-resolved densities of states (DOS) at the Fermi level are proportional to the tunneling current and use them in the definition of P instead of conductance G, we obtain the negative values of P for Co and Ni, which is in obvious disagreement with the experiments.[2] Therefore, it becomes clear that the simple interpretation of the spin-polarized tunneling based on spin densities of states does not provide a clear explanation of experimental observations and we must take into account the fact the transmission probabilities for different electronic states make substantially different contributions to the tunneling current. This conclusion is supported by a number of first-principles calculations of spin-polarized tunneling for ideal MTJs with vacuum or epitaxial barriers.[3] Qualitatively, the difference in the transmission probabilities is explained by the fact that different electronic states have different symmetries, which results in the appearance of certain selection rules related to the complex band structure of the barrier.[4] For example, it is often stated that 3*d* states of a ferromagnet cannot tunnel into the alumina barrier because there are no *d* states in it to couple with *d* states of the electrodes. As a result, only the *s* component of the electrode DOS is said to contribute to the tunneling current. This quantity is often referred to as the "tunneling DOS."[5]

The above argument suggests an intuitive explanation of the fact that the P and DOS ratios need not be equal, but from the quantitative point of view it is clearly insufficient. Indeed, there is no general rule that forbids the Bloch states composed predominantly of *d* orbitals to tunnel through the barrier with no *d* orbitals. Symmetry strictly forbids tunneling only in systems with special geometries and for special values of the wave vector. In a particular MTJ, these selec-

tion rules may or may not compensate for the negative DOS ratio.

The actual picture is even more complex. In reality, the atomic and electronic structure of the interface between the ferromagnet and the insulator may strongly affect the transmission probabilities.[6] In particular, we have recently found[7] that the spin polarization of the clean Co (111) surface is large and *negative*, but the deposition of a monolayer of oxygen makes it positive and close to 100%. This reversal is due to the interface bonding between Co and O atoms, which results in the formation of an interface band of states which mix differently with bulk states for up-spin and down-spin channels and even involve additional selection rules for tunneling. Therefore, it is clear that the interfaces strongly influence the spin polarization and TMR of magnetic tunnel junctions. The effect of interfacial structure and disorder on the tunneling spin polarization and spin injection was also noted in Refs. 8 and 9.

In this paper we study spin-dependent tunneling in $Co/Al_2O_3/Co$ MTJs using first-principles Green's function description of the electron transport. We assume crystalline epitaxy at the interface between Co and Al_2O_3 and consider two fully relaxed atomic configurations of the O-terminated interface that differ only by the presence or absence of an adsorbed oxygen atom at the interface. We show that these structures exhibit opposite signs of the spin polarization of the tunneling current, reflecting features of the electronic structure and bonding at the Co/Al_2O_3 interface and, thereby, evidencing the crucial role of the interface in controlling the spin polarization.

II. ATOMIC STRUCTURE OF THE INTERFACES

The first model represents the O-terminated $Co/Al_2O_3/Co$ structure obtained in Ref. 10. The interface structure for this model (model 1) is shown in Figs. 1(a) and 1(b). The lateral dimensions of the supercell correspond to a 2×2 surface unit cell of the (111) plane of fcc Co. The (0001)-oriented corundum lattice of Al_2O_3 has seven monolayers: Four O layers with three O atoms in each layer, and three Al layers with two Al atoms in each layer (not shown). This structure has a 6% lattice mismatch between Co and Al_2O_3. The interface contains three oxygen atoms per unit cell. The oxygen atoms are located close to the bridge adsorption sites of the Co surface. These oxygen atoms participate in bonding with the two adjacent Al atoms, making the bonds of the latter fully saturated.

Inspection of model 1 reveals the presence of a rather large pore at one of the three-fold hollow adsorption sites above the Co surface. The second model (model 2) is obtained by adding an O atom [referred to as O(II)] into this pore, followed by complete structural relaxation, which was performed using the pseudopotential plane-wave method[11] within the generalized gradient approximation. The interface structure for model 2 is shown in Figs. 1(c) and 1(d). Notably, the three O(I) atoms in the relaxed model 2 structure move away from the bridge sites toward the three-fold hollow sites. The rippling of the Co surface layer, which is about 0.2 Å in model 1, almost completely disappears in model 2. However, in model 2 the oxygen layer becomes rippled, the additional O(II) atom being much closer to its three Co(II) neighbors compared to the O(I) atoms. The length of Co(II)-O(II) bonds is 1.79 Å, compared to the three inequivalent bond lengths of 2.05, 2.18, and 2.24 Å formed by O(I) atoms with different Co atoms. The position of the O(II) atom in the three-fold hollow site above the three Co(II) atoms is very close to the position of O atoms in the adsorbed monolayer,[7] the Co-O bond lengths being 1.82 Å. This fact reflects a very strong bonding of this O(II) atom to the Co surface.

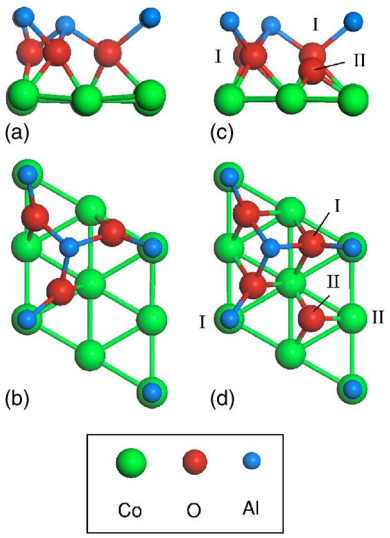

FIG. 1. Interfacial structure for model 1 (a), (b) and model 2 (c), (d). Panels (a), (c) show "front" views from a direction normal to the three-fold axis; panels (b), (d) show "top" views along the three-fold axis. There are two types of Co and O atoms at the interface for model 2: three O(I) atoms, one O(II) atom, one Co(I) atom, and three Co(II) atoms per unit cell.

III. SPIN-POLARIZED TUNNELING

For both MTJ models we have calculated the transmission functions for the parallel orientation of electrodes using the principal-layer Green's function approach[12] based on the tight-binding linear muffin-tin orbital method (TB-LMTO) in the atomic sphere approximation (ASA), and the transmission matrix formulation of Ref. 13. Local density approximation (LDA) was used in all calculations. All atomic potentials were determined self-consistently using the supercell approach within the TB-LMTO-ASA method.

To quantify the spin asymmetry of the tunnel junction, we calculated the total conductances $G_\uparrow$ and $G_\downarrow$ in the parallel configuration for the majority- and minority-spin channel, respectively. The total tunneling current for model 1 is polarized negatively with the conductances $G_\uparrow=0.0042e^2/h$ and $G_\downarrow=0.023e^2/h$ per cell area, which corresponds to the spin polarization of -70%. Note that, although this quantity is not directly measurable, it correlates with the measurable spin polarization P.

Qualitatively this result is similar to the case of the pure Co (111) surface, showing the dominant contribution of the

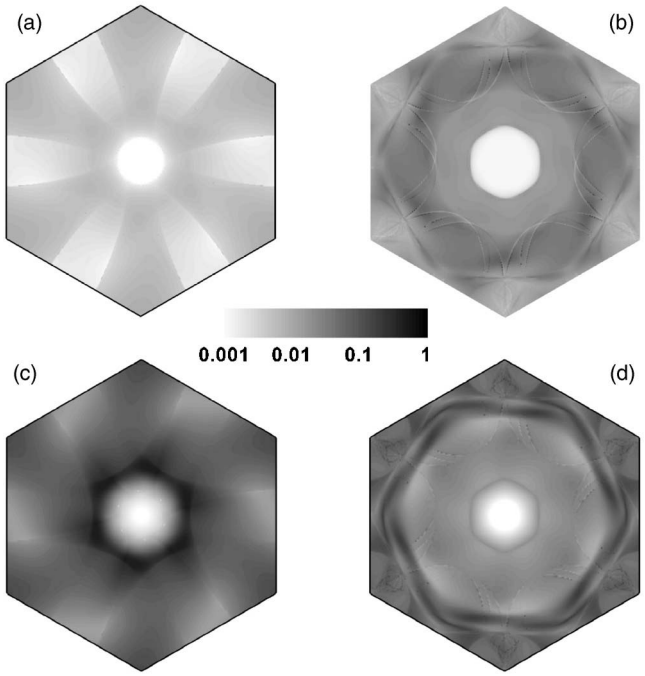

FIG. 2. $\mathbf{k}_\parallel$-resolved transmission in units of e^2/h (logarithmic scale) in $Co/Al_2O_3/Co$ tunnel junctions with different interface structures. (a), (b) model 1; (c), (d) model 2. (a), (c) Majority spin; (b), (d) minority spin.

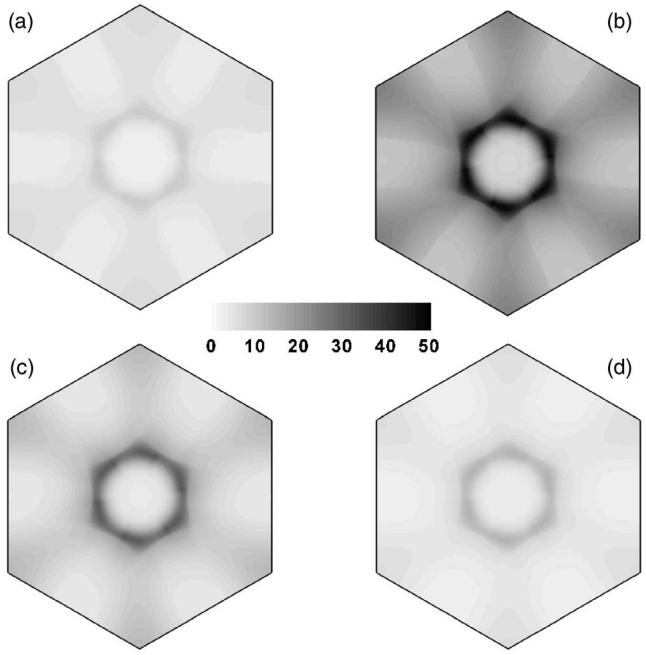

FIG. 3. $\mathbf{k}_\parallel$-resolved majority-spin densities of states at the Fermi level for different atoms at the Co/Al_2O_3 interface for model 2. (a) Co(I), (b) Co(II), (c) O(II), and (d) O(I). All values are given per atom of the given type. The units are arbitrary.

minority-spin conductance when tunneling occurs through vacuum.[7] This analogy is not coincidental because it reflects a relatively weak bonding between O and Co atoms in the structure of model 1 compared to model 2. The latter fact can be understood by analyzing the local DOS shown in Fig. 4 of Ref. 10. The local DOS of the interface Co and O atoms are quite similar to those in the bulk of the Co electrode and the Al_2O_3 barrier respectively. Just as in the case of the vacuum barrier, the bulk states remain metallic up to the interface Co layer, while the local DOS of the oxide layer is very similar to that in the bulk of Al_2O_3. The relatively weak bonding between the Co and O atoms at the interface also results in the rotation of these O atoms from the three-fold hollow positions on the Co surface toward the equilibrium positions in the bulk Al_2O_3 structure. Thus, it is the weak bonding between the Co electrode and the oxide barrier that is responsible for the negative spin polarization of the tunneling current in model 1.

This situation changes dramatically when an additional O atom is placed at the interface. We found that model 2 exhibits a reversal of the spin polarization from negative to positive. The total conductances are $G_\uparrow = 0.087 e^2/h$ and $G_\downarrow = 0.045 e^2/h$ per cell area, and the spin polarization is +32%. This is similar to the vacuum barrier case, showing that the deposition of a monolayer of O on the Co (111) reverses the spin polarization compared to the pure Co surface.[7] However, the mechanism of the reversal in the case of the Al_2O_3 barrier is somewhat different and is discussed in detail below.

Figure 2 shows the calculated $\mathbf{k}_\parallel$-resolved transmission functions. We see that the minority-spin transmission functions [panels (b) and (d)] are qualitatively similar for both models, the tunneling current being appreciable through most of the interface Brillouin zone (IBZ) with more weight at the periphery. The central area with very small transmission reflects the presence of a hole in one of the Fermi surface sheets that dominates the conductance.

The situation is different for majority-spin states. For model 1 (panel a) the transmission function is again significant throughout the entire IBZ except for the circular region around the Γ point (corresponding to the hole in the majority-spin Fermi surface). The features of the transmission function reflect the shape of the Fermi surface folded down into the IBZ for the given supercell. However, for model 2 [panel (c)] we observe that the tunneling current is dominated by a rather narrow hexagonally shaped region encircling the central region of the low conductance. (The logarithmic scale under-represents this domination.) The fact that this feature appears with the addition of an O atom at the interface suggests that it is induced by new interface states. This is confirmed by the plots of the $\mathbf{k}_\parallel$-resolved local DOS for the respective atoms at the interface shown in Fig. 3. We clearly see that the hexagonal feature in the majority-spin transmission function corresponds to high DOS at Co(II) and O(II) atoms which "leaks" weakly to the neighboring atoms. The hexagonal feature has a significant width, which indicates a significant overlap between the interface and the bulk Bloch states.

As it was mentioned above, Co(II) and O(II) atoms are positioned very similar to the Co and O atoms at the Co (111) surface with an adsorbed oxygen monolayer. Just as in that case, Co(II) and O(II) atoms in model 2 form bonding and antibonding orbitals which are clearly seen in the local DOS plots shown in Fig. 4. The bonding states lie below the

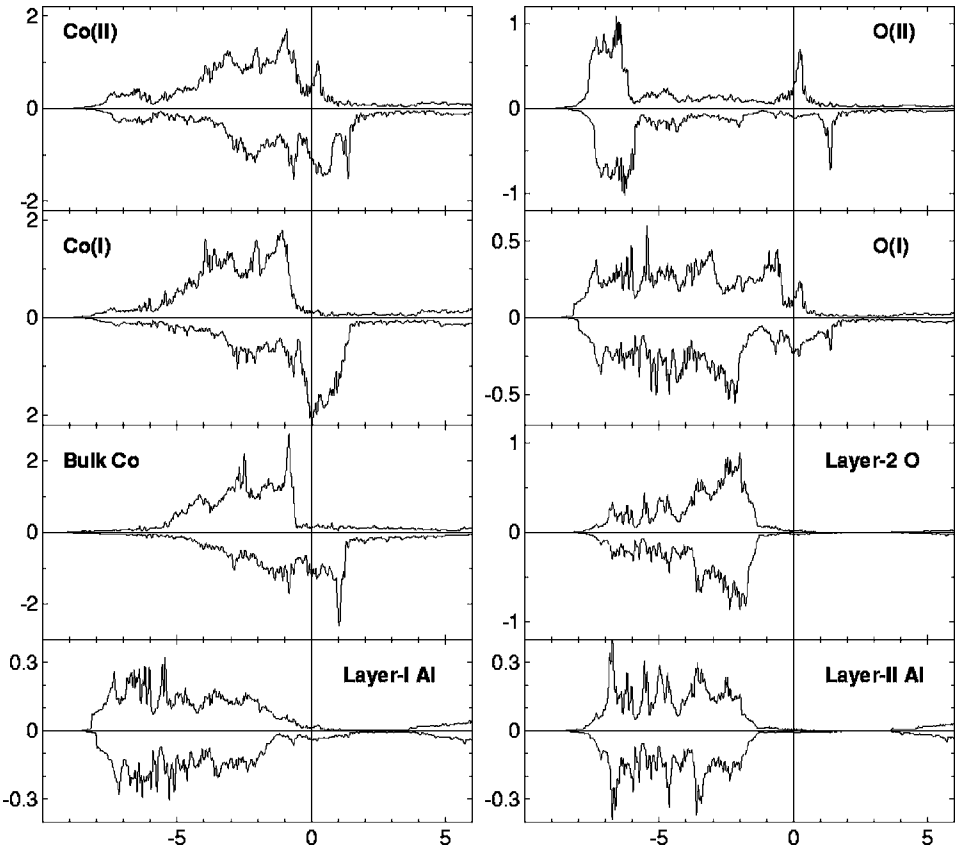

FIG. 4. Partial densities of states for model 2. Energy is in electron volts, DOS is in electron volts^{-1} per atom. Co(I), Co(II), O(I), and O(II) atoms are at the Co/Al_2O_3 interface (see Fig. 1). Layer numbers for other atoms increase into the barrier. For example, Layer-II Al is just in the middle of the barrier. Layer-I Al DOS is the average of those for two inequivalent Al atoms in this layer.

bottom of the Co 3*d* band, while the antibonding states are slightly above the Fermi level. Some of the DOS weight is removed from the Fermi level to these hybridized states, so that the Stoner criterion for Co(II) atoms is weakened. The magnetic moments at the interface layer are 2.09 μ_B for Co(I) and 1.30 μ_B for Co(II). While the magnetic moment of Co(II) atoms is notably reduced, this effect is much smaller compared to the oxidized surface, because in model 2 there is only one "adsorbed" O(II) atom per three Co(II) atoms. It is clearly seen in Fig. 4 that the antibonding interface states are exchange split by nearly 1 eV.

Thus, we see that the surface or interface adsorption of O atoms in the three-fold hollow sites reverses the sign of the spin polarization of the tunneling current due to the bonding of the adsorbed O atoms with Co. However, the mechanism of this reversal in these two cases of Co/vacuum and Co/Al_2O_3 is different. For the oxidized surface, Co-O bonding removes the conducting orbitals that form the bulk Bloch states from the surface Co and O layers at the Fermi level, and essentially create an additional tunneling barrier positioned at these layers. In the case of partial coverage as in model 2 this effect is limited to O(II) atoms which can be seen from the $\mathbf{k}_\parallel$-resolved transmission function for minority-spin electrons (not shown). Therefore, the conductance through O(I) atoms is not blocked. The main effect of the interface adsorption is obviously in the majority-spin channel, where the conductance is enhanced 20-fold compared to model 1. This increase is due to the fact that the antibonding Co-O states are present at the Fermi level, moderately mix with the bulk states, and form the interface resonances which strongly assist the tunneling. At the same time, the minority-spin antibonding Co-O states in model 2 lie more than 1 eV higher in energy due to exchange splitting (see Fig. 4) and do not affect the conductance. A similar mechanism of reversal of the spin polarization of the local DOS was found for the oxidized Fe(001) surface.[14]

IV. TUNNELING MAGNETORESISTANCE

Let us now consider the tunneling magnetoresistance for two models considered in the paper. We calculated the conductance for antiparallel orientation of magnetization of the two electrodes using the atomic potentials obtained for the parallel orientation. The spin-up and spin-down potentials were simply exchanged for all atoms on one side of the central plane of the barrier. For model 1 the tunneling current for each spin channel in the antiparallel orientation is $0.0082e^2/h$ per cell area, which gives the TMR of 66%. For model 2, the tunneling current for the antiparallel orientation is $0.040e^2/h$ per cell area, the TMR is 65%. As we saw above, the role of spin channels is now reversed, therefore, the similarity of TMR values for both models is obviously a coincidence.

We have shown in Ref. 7 that for a sufficiently thick barrier, the transmission function factorizes into a product of two surface transmission functions and a spin-independent barrier decay factor. This factorization takes place under the condition that the tunneling eigenstate for each $\mathbf{k}_\parallel$ is dominated by one barrier eigenstate with the smallest decay parameter, and the multiple scattering across the barrier may be neglected. In this limit, the conductance per spin channel for antiparallel configuration $G_{\uparrow\downarrow}$ is the geometrical mean of the

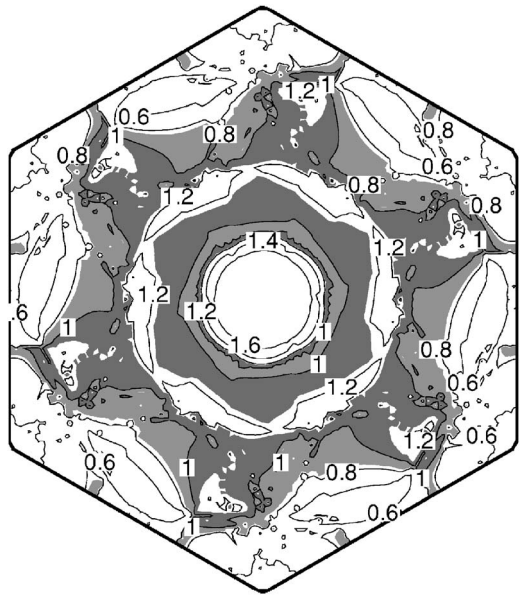

FIG. 5. Quality factor (see text) for model 1 plotted in the surface Brillouin zone. $Q=1$ corresponds to factorizing transmission. Gray shading shows the region where $0.85<Q<1.15$.

spin-up and spin-down conductances obtained for the parallel configuration: $G_{\uparrow\downarrow}(\mathbf{k}_\parallel)=\sqrt{G_{\uparrow\uparrow}(\mathbf{k}_\parallel)G_{\downarrow\downarrow}(\mathbf{k}_\parallel)}$. It is interesting to study to what extent this factorization survives in the present case of a rather thin Al_2O_3 barrier, which also has a much higher transparency compared to the vacuum barrier considered in Ref. 7. To this end, we calculate a "quality factor" $Q(\mathbf{k}_\parallel)=G_{\uparrow\downarrow}/\sqrt{G_{\uparrow\uparrow}G_{\downarrow\downarrow}}$ which is close to 1 if the factorization of the transmission takes place.

The plot of the quality factor for model 1 is shown in Fig. 5. As we see, in a large fraction of the surface Brillouin zone the quality factor significantly deviates from 1, which means that the transmission function does not factorize. The reason for this becomes clear from Fig. 6 which shows the five smallest decay parameters (imaginary parts of wave vectors) of the Al_2O_3 eigenstates, along the two directions in the surface Brillouin zone of the MTJ. The complex wave vectors were calculated using the technique of Ref. 15.

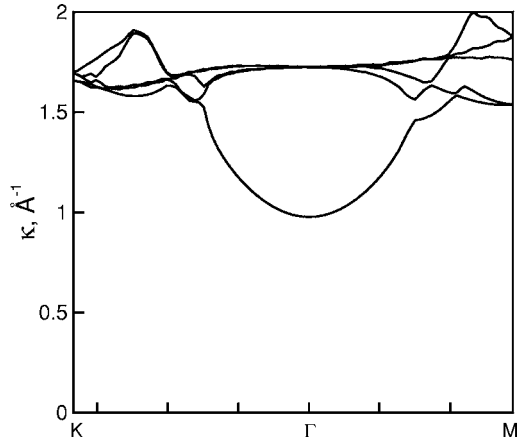

FIG. 6. Five smallest imaginary parts of the eigenstate wave vectors of Al_2O_3 strained to the epitaxy of model 1.

We see from Fig. 6 that the lowest parabolic branch in the central part of the surface Brillouin zone is well separated from the states with larger values of κ. Therefore, the assumption of a single dominant evanescent wave for the given value of $\mathbf{k}_\parallel$ may be reasonable in this region. The inspection of the smallest decay parameters between the ΓK and ΓM lines (not shown) reveals that the gap between the smallest and the next smallest decay parameters also somewhat widens at the periphery of the surface Brillouin zone, so that the factorization may survive in those regions as well. Both these conclusions are generally corroborated by Fig. 5, where the shaded areas show the regions with the quality factor close to 1. However, there is a significant discrepancy in the vicinity of the Γ point where the quality factor is close to 3. The analysis of the layer- and $\mathbf{k}_\parallel$-resolved DOS for the MTJ reveals that the metal-induced DOS decays faster in this region compared to the shaded areas in Fig. 5. The reason for this "anomaly" around the Γ point lies in the symmetry of the MTJ. Although model 1 contains four Co atoms per each layer in the unit cell, the higher symmetry of a unit cell with one Co atom per cell is broken only moderately. Therefore, although the selection rules enforced by that higher symmetry are no longer exact, they are still obeyed approximately.

The states around the Γ point in the minority-spin channel come from the corners of the original surface Brillouin zone for the cell with one Co atom per layer (see Ref. 7). If the higher symmetry were fully retained, the Fourier expansion of the eigenstates at the Γ point in our MTJ cell would start from nonzero reciprocal lattice vectors $\mathbf{G}_i$, and these states would be orthogonal to the barrier eigenstate with the smallest decay parameter (the lowest parabolic branch in Fig. 6). In our case of relaxed symmetry, and away from the Γ point, the tunneling eigenstates have a component with $\mathbf{G}=0$, but it is numerically small compared to those with $\mathbf{G}\neq 0$. Therefore, to reach the limit of factorizing transmission function, the barrier should be very thick so that the components with $\mathbf{G}\neq 0$ decay to zero and leave only the one with $\mathbf{G}=0$ which is originally much smaller. The barrier in our model 1 is not sufficiently thick for this to happen, and this is the source of the Γ point anomaly seen in Fig. 5. Thus, we see that although the factorization of the tunneling conductance discussed in Ref. 7 is approximately valid in some areas of the surface Brillouin zone, it cannot be used for calculation of magnetoresistance of MTJs containing just a few atomic layers of the insulating barrier. The situation is even worse for model 2, where the transmission function reaches rather high values, and hence multiple scattering across the barrier becomes important.

V. DISCUSSION

We have shown in this paper that the addition of interfacially adsorbed oxygen in model 2 reverses the spin polarization of the tunneling current from negative to positive due to the appearance of new current paths passing through O(II) atoms which act as positive spin filters. Although it is unclear to what extent our models 1 and 2 reflect the real structure of the Co/Al_2O_3 interfaces in MTJs, chemical intuition suggests that the oxide next to the interfaces should be rather

friable. Because the O(II) atoms in model 2 demonstrate strong bonding with Co surface and weak bonding with other atoms of the oxide, it is reasonable to assume that excess oxygen will be adsorbed on the Co surface at three-fold adsorption sites inside the available pores. Qualitatively, one may consider a "two-component model" where the total tunneling current is the sum of positively polarized current through adsorbed oxygen atoms and negatively polarized current through other oxygen atoms. The resulting spin polarization will obviously depend on the amount of adsorbed oxygen, which is controlled by specific growth conditions.

Within our crystalline barrier model, taking into account the complex band structure shown in Fig. 6, the tunneling current should decrease slower with increasing barrier thickness when it is carried by states with small $\mathbf{k}_{\|}$. As it is clear from Figs. 2 and 3, current through O(II) atoms is carried by states which are rather close to the zone center, while the current in model 1 is distributed over the entire zone. Therefore, the spin polarization in model 2 should increase with barrier thickness. Qualitatively similar behavior was recently observed in Meservey-Tedrow measurements of the spin polarization as a function of Al_2O_3 barrier thickness.[16]

We have seen that O adsorption at the Co/Al_2O_3 interface results in a reduction of the magnetic moment of Co atoms that are bound to the adsorbed atoms O(II). As a result, Co atoms with different magnetic moments may exist on the real Co/Al_2O_3 interface containing a certain amount of adsorbed oxygen. In principle, these magnetic moments may be probed experimentally. The work of Telling *et al.*[17] shows that the Co spin polarization at the interface with Al_2O_3 strongly correlates with the TMR, suggesting that interface bonding is indeed a controlling factor for the high TMR in alumina-based tunnel junctions.

In conclusion, we have considered spin-polarized tunneling in crystalline $Co/Al_2O_3/Co$ tunnel junctions within the first-principles Green's function approach. We distinguished two types of the interface O atoms: those that saturate Al bonds and the those that are adsorbed by Co. The latter bind strongly to Co producing spin-dependent interface states which enhance the tunneling current in the majority-spin channel, thus making the spin polarization of the conductance positive. This fact suggests that the common argument of the dominant *s*-electron contribution to tunneling, which is often used to explain the positive spin polarization of the alumina-based tunnel junctions is not fully justified. We showed that the spin polarization in Co/alumina/Co MTJs is controlled by the interfacial atomic structure and resulting chemical bonding. Moreover, the interfacial adsorption of oxygen may be the major factor resulting in the positive spin polarization as is observed in experiment. Our results indicate that the control of oxidation of the ferromagnetic layer in alumina-based tunnel junctions is of paramount importance for achieving substantial values of the spin polarization of the tunneling current.

ACKNOWLEDGMENTS

The work at UNL was supported by NSF (DMR-0203359 and MRSEC DMR-0213808) and the Nebraska Research Initiative. I.I.O. was supported by NSF (CCF-0432121). M.vS. was supported by the Office of Naval Research. The calculations were performed using the Research Computing Facility of the University of Nebraska-Lincoln.

[1] E. Y. Tsymbal, O. N. Mryasov, and P. R. LeClair, J. Phys.: Condens. Matter **15**, R109 (2003).
[2] R. Meservey and P. M. Tedrow, Phys. Rep. **238**, 173 (1994).
[3] X.-G. Zhang and W. H. Butler, J. Phys.: Condens. Matter **15**, R1603 (2003).
[4] Ph. Mavropoulos, N. Papanikolaou, and P. H. Dederichs, Phys. Rev. Lett. **85**, 1088 (2000).
[5] M. B. Stearns, J. Magn. Magn. Mater. **5**, 1062 (1977).
[6] E. Y. Tsymbal and D. G. Pettifor, J. Phys.: Condens. Matter **9**, L411 (1997).
[7] K. D. Belashchenko, E. Y. Tsymbal, M. van Schilfgaarde, D. A. Stewart, I. I. Oleinik, and S. S. Jaswal, Phys. Rev. B **69**, 174408 (2004).
[8] X.-G. Zhang, W. H. Butler, and A. Bandyopadhyay, Phys. Rev. B **68**, 092402 (2003).
[9] M. Zwierzycki, K. Xia, P. J. Kelly, G. E. W. Bauer, and I. Turek, Phys. Rev. B **67**, 092401 (2003).
[10] I. I. Oleinik, E. Y. Tsymbal, and D. G. Pettifor, Phys. Rev. B **62**, 3952 (2000).
[11] M. C. Payne, M. P. Teter, D. C. Allan, T. A. Arias, and J. D. Joannopoulos, Rev. Mod. Phys. **64**, 1045 (1992).
[12] I. Turek, V. Drchal, J. Kudrnovský, M. Šob, and P. Weinberger, *Electronic Structure of Disordered Alloys, Surfaces and Interfaces* (Kluwer, Boston, 1997).
[13] J. Kudrnovský, V. Drchal, C. Blaas, P. Weinberger, I. Turek, and P. Bruno, Phys. Rev. B **62**, 15084 (2000).
[14] E. Y. Tsymbal, I. I. Oleinik, and D. G. Pettifor, J. Appl. Phys. **87**, 5230 (2000).
[15] A.-B. Chen, Y.-M. Lai-Hsu, and W. Chen, Phys. Rev. B **39**, 923 (1989).
[16] M. Münzenberg and J. S. Moodera, Phys. Rev. B **70**, 060402(R) (2004).
[17] N. D. Telling, G. van der Laan, S. Ladak, and R. J. Hicken, Appl. Phys. Lett. **85**, 3803 (2004).